

The first quantitative estimation of the influence of volcanic activity on noctilucent clouds

Peter A. Dalin¹, Nikolay Pertsev², Vladimir Perminov², and Vitaly Romejko³

¹Swedish Institute of Space Physics

²A. M. Obukhov Institute of Atmospheric Physics, RAS

³The Moscow Association for NLC Research

November 22, 2022

Abstract

Climate change happening in the middle and upper atmosphere has been intensively investigating nowadays. One of the experimental tools to investigate long-term changes in the mesopause region between 80 and 90 km altitude is a natural atmospheric phenomenon called noctilucent clouds (NLCs). Being composed of tiny ice particles, NLCs are supposed to be highly sensitive to small changes in the temperature and amount of water vapor at the polar summer mesopause. Many factors such as solar activity, long-term changes in the temperature, amount of water vapor, minor atmospheric constituents, have been considered contributing to long-term NLC changes. At the same time, a role of volcanic activity in the NLC variability has been investigated in a qualitative sense in previous studies so far, and its influence has been found to be inconclusive. For the first time, we quantitatively investigate a factor of volcanic activity in NLC variability for the past five decades. Our analysis reveals that there is statistically significant positive influence of volcanic activity on changes in NLC activity, with a time lag of 7 years between these processes which might be explained by a slow meridional-vertical updraft of ejected volcanic water vapor from the tropical troposphere to the polar mesopause region. We confirm our previous results on no statistically significant long-term trend in NLC activity at middle and subpolar latitudes for the past five decades.

Table 1 . Regression coefficients of the multiple regression model (see equation 1), along with their standard deviations (1.5 or 2 or 3 standard deviations) for the NLC occurrence number and NLC brightness for the period of 1968-2018. Corresponding confidence probabilities (90% or 95% or 99%) are shown in brackets. Statistically significant coefficients (equal to or greater than its error) at the corresponding confidence levels are marked in bold. The time regression coefficient (C_1) is expressed in value per year (V/yr), the solar regression coefficient (C_2) is expressed in value per solar flux unit (SFU, 10^{11} photons $\text{cm}^{-2}\text{s}^{-1}$), the volcanic regression coefficient (C_3) is expressed in value per VEI (Value/VEI), C_0 is the regression constant. Phase lags (years) are introduced for the Lyman α flux and VEI. The P values for the null hypothesis test have been calculated for each regression coefficient. Table 1 represents three model runs with three different selections of volcanic activity:

- a) all volcanic eruptions that occurred around the world (all VEI values, all longitudes and all latitudes);
 - b) volcanic eruptions with all VEI values at all longitudes and at latitudes between 30°S and 30°N;
 - c) volcanic eruptions with VEI \geq 3 at all longitudes and at latitudes between 30°S and 30°N.
- (a) All volcanic eruptions (all VEI, all longitudes and all latitudes)

C_0 (V)	C_1 (V/yr)	C_1 (V/yr)	C_2 (V/SFU) and lag (yr)	C_3 (V/VEI) and lag (yr)
-----------	--------------	--------------	-------------------------------	-------------------------------

NLC occurrence number	40.0±14.1 (99%), P=0.0	-0.003±0.087 (90%), P=0.960	-0.003±0.087 (90%), P=0.960	-2.066±1.831 (95%), lag=0, P=0.028	0.105±0.083 (90%), lag=7, P=0.038
NLC brightness	111.1±44.3 (99%), P=0.0	0.159±0.272 (90%), P=0.330	0.159±0.272 (90%), P=0.330	-8.599±7.673 (99%), lag=0, P=0.004	0.305±0.259 (90%), lag=7, P=0.054
(b) Volcanoes with all VEI, all longitudes and latitudes between 30°S and 30°N	(b) Volcanoes with all VEI, all longitudes and latitudes between 30°S and 30°N	(b) Volcanoes with all VEI, all longitudes and latitudes between 30°S and 30°N	(b) Volcanoes with all VEI, all longitudes and latitudes between 30°S and 30°N	(b) Volcanoes with all VEI, all longitudes and latitudes between 30°S and 30°N	(b) Volcanoes with all VEI, all longitudes and latitudes between 30°S and 30°N
NLC occurrence number	41.8±12.6 (99%), P=0.0	-0.027±0.089 (90%), P=0.619	-0.027±0.089 (90%), P=0.619	-2.145±1.793 (95%), lag=0, P=0.020	0.152±0.122 (95%), lag=7, P=0.016
NLC brightness	117.3±39.9 (99%), P=0.0	0.102±0.284 (90%), P=0.549	-8.832±7.615 (99%), lag=0, P=0.003	-8.832±7.615 (99%), lag=0, P=0.003	0.406±0.387 (95%), lag=7, P=0.040
(c) Volcanoes with VEI>=3, all longitudes and latitudes between 30°S and 30°N	(c) Volcanoes with VEI>=3, all longitudes and latitudes between 30°S and 30°N	(c) Volcanoes with VEI>=3, all longitudes and latitudes between 30°S and 30°N	(c) Volcanoes with VEI>=3, all longitudes and latitudes between 30°S and 30°N	(c) Volcanoes with VEI>=3, all longitudes and latitudes between 30°S and 30°N	(c) Volcanoes with VEI>=3, all longitudes and latitudes between 30°S and 30°N
NLC occurrence number	44.7±11.5 (99%), P=0.0	-0.021±0.084 (90%), P=0.674	-2.359±2.345 (99%), lag=0, P=0.010	-2.359±2.345 (99%), lag=0, P=0.010	0.373±0.339 (99%), lag=7, P=0.005
NLC brightness	124.8±36.4 (99%), P=0.0	0.106±0.267 (90%), P=0.506	-9.442±7.409 (99%), lag=0, P=0.001	-9.442±7.409 (99%), lag=0, P=0.001	1.070±1.071 (99%), lag=7, P=0.010

1 **The first quantitative estimation of the influence of volcanic**
2 **activity on noctilucent clouds**

3
4 Peter Dalin^{1,2*}, Nikolay Pertsev³, Vladimir Perminov³, & Vitaly Romejko⁴

5
6 ¹Swedish Institute of Space Physics, Box 812, SE-981 28 Kiruna, Sweden

7 ²Space Research Institute, RAS, Profsovnaya st. 84/32, Moscow, 117997, Russia

8 ³A.M. Obukhov Institute of Atmospheric Physics, RAS, Pyzhevskiy per. 3, Moscow, 119017,
9 Russia

10 ⁴The Moscow Association for NLC Research, Kosygina st. 17, Moscow, 119334,
11 Russia

12
13 *Corresponding author at: Swedish Institute of Space Physics, Box 812, SE-981 28
14 Kiruna, Sweden. Fax: +46 980 79050. E-mail address: pdalin@irf.se (P. Dalin).

15
16 **Abstract**

17 Climate change happening in the middle and upper atmosphere has been intensively
18 investigating nowadays. One of the experimental tools to investigate long-term
19 changes in the mesopause region between 80 and 90 km altitude is a natural
20 atmospheric phenomenon called noctilucent clouds (NLCs). Being composed of tiny
21 ice particles, NLCs are supposed to be highly sensitive to small changes in the
22 temperature and amount of water vapor at the polar summer mesopause. Many factors
23 such as solar activity, long-term changes in the temperature, amount of water vapor,
24 minor atmospheric constituents, have been considered contributing to long-term NLC
25 changes. At the same time, a role of volcanic activity in the NLC variability has been
26 investigated in a qualitative sense in previous studies so far, and its influence has been
27 found to be inconclusive. For the first time, we quantitatively investigate a factor of
28 volcanic activity in NLC variability for the past five decades. Our analysis reveals that
29 there is statistically significant positive influence of volcanic activity on changes in
30 NLC activity, with a time lag of 7 years between these processes which might be
31 explained by a slow meridional-vertical updraft of ejected volcanic water vapor from
32 the tropical troposphere to the polar mesopause region. We confirm our previous

33 results on no statistically significant long-term trend in NLC activity at middle and
34 subpolar latitudes for the past five decades.

35

36 **1. Introduction**

37 Spectacular night-shining clouds or noctilucent clouds (NLCs) are the highest
38 clouds in the Earth's atmosphere observed at the summer mesopause between 80 and
39 90 km. NLCs can be readily seen from mid- and subpolar latitudes of both
40 hemispheres. NLCs are composed of water-ice particles of 30–100 nm in radius that
41 scatter sunlight and thus NLCs are observed against the dark twilight arc from May
42 until September in the Northern Hemisphere and from November to February in the
43 Southern Hemisphere (Bronshten & Grishin, 1970; Gadsden & Schröder, 1989).
44 NLCs are also observed from space and in this case they are usually called Polar
45 Mesospheric Clouds, PMCs (Thomas, 1984).

46 A small size of NLC ice particles makes them a perfect natural indicator of
47 potential climate change happening in the middle atmosphere. For comparison
48 purposes note that ice particles of cirrus tropospheric clouds are by one-four orders of
49 magnitude greater than NLC ice crystals (Kärcher et al., 2014). Since 1990s, there is a
50 growing interest in studies of long-term time series of NLCs/PMCs (Berger &
51 Lübken, 2015; Dalin et al., 2006, 2020; DeLand et al., 2006, 2015, 2019; Dubietis et
52 al., 2010; Fiedler et al., 2017; Gadsden, 1990, 1997; Hervig & Siskind, 2006;
53 Kirkwood et al., 2003, 2008; Lübken & Berger, 2011; Lübken et al., 2018; Pertsev et
54 al., 2014; Romejko et al., 2003; Shettle et al., 2009; Zalcik et al., 2016). Up to now,
55 various methods (model simulations, ground-based NLC observations, PMC
56 measurements from space) show various results on long-term trends in NLC/PMC
57 activity, which demonstrate the complexity of the problem (Dalin et al., 2020).
58 However, in order to retrieve correct information on long-term changes in NLCs one
59 needs to separate their long-term changes in time from other solar-geophysical
60 processes having interannual and decadal variabilities. Thus, the 11-year solar cycle,
61 interannual and long-term variations in the content of water vapor, ozone, carbon
62 dioxide and methane have been considered in a wealth of papers dealing with long-
63 term trends in NLCs/PMCs (Berger & Lübken, 2015; Dalin et al., 2020; DeLand et
64 al., 2015, 2019; Fiedler et al., 2017; Hervig & Siskind, 2006; Lübken & Berger, 2011;
65 Lübken et al., 2018; Pertsev et al., 2014). However, a volcanic factor as a driver of
66 variability in the NLC activity has been scantily addressed so far, mainly by

67 qualitatively considering major volcanic eruptions only (Bronshen & Grishin, 1970;
68 Gadsden & Schröder, 1989; Fogle & Haurwitz, 1973; Hervig et al., 2016; Thomas &
69 Olivero, 2001; Thomas et al., 1989). It has been found that after some major eruptions
70 (Krakatoa in 1883, Bezymianny in 1956, Agung in 1963) there was an increase in
71 NLC activity whereas other volcanic events (Okataina in 1886, Mount Pelée and
72 Santa Maria in 1902, Tarumai in 1909, Taal in 1911, Katmai in 1912) did not result in
73 increased NLC activity (Bronshen & Grishin, 1970; Dalin et al., 2012; Fogle &
74 Haurwitz, 1973; Gadsden & Schröder, 1989; Thomas & Olivero, 2001). In general,
75 conflicting evidences of the influence of volcanic activity on NLC activity have been
76 obtained (Fogle & Haurwitz, 1973). In a recently published paper (Lübken et al.,
77 2018) dealing with model studies of long-term trends in NLCs, the authors have noted
78 that the role of volcanic eruptions for long-term evolution of NLCs should be
79 addressed in more detail. This motivated us to reinvestigate a volcanic factor as a
80 potential driver for long-term evolution of NLCs based, for the first time, on high
81 quality long-term data series of NLC and volcanic activities as well as using a robust
82 statistical method of the present analysis.

83

84 **2. Data Source**

85 Long-term data series of NLC observations conducted in the Moscow region in
86 Russia (~56°N, 37°E) for the period of 1968-2018 have been used. The full Moscow
87 NLC database analyzed in the present paper is available at the project website:
88 http://ifaran.ru/lab/lfva/NLC_data_engl.html. We utilize two parameters
89 characterizing yearly NLC activity: the NLC occurrence number and NLC brightness.
90 The full description of the NLC database, method of observations and estimated
91 parameters can be found in Romejko et al. (2003) and Dalin et al. (2020).

92 Time series of the Lyman α flux at 121.6 nm as a proxy of solar activity have been
93 utilized for the period of 1968-2018, which were obtained from the LASP Interactive
94 Solar Irradiance Datacenter (LISIRD) available at <http://lasp.colorado.edu/lisird>.

95 We have used quantitative information on global volcanic activity for the past five
96 decades available at the Global Volcanism Program of the Smithsonian Institute
97 (http://volcano.si.edu/search_eruption.cfm#). Volcanic eruptions are classified by the
98 Volcanic Explosivity Index (VEI) that describes the magnitude of an explosive
99 volcanic eruption. The VEI scale extends from 0 to 8 marks, representing a
100 logarithmic scale in which an increase of 1 unit corresponds to an increase of intensity

101 of a factor of 10. VEI includes the following eruption characteristics: total volume of
102 explosive products, height of eruptive cloud above the vent, eruption type, duration of
103 continuous blast, extent of tropospheric and stratospheric injection and some other
104 descriptive characteristics (Newhall & Self, 1982; Siebert et al., 2010).

105 Since several tens of volcanic eruptions occur each year, we have made the
106 following processing of the VEI value in order to make it comparable to yearly
107 numbers of the NLC activity:

108 a) each volcanic year has been defined from May to May of two successive
109 calendar years. This is due to the fact NLCs start to be visible from late May at middle
110 latitudes.

111 b) the sum of all VEI values has been calculated for each volcanic year, i.e., we
112 define and analyze the total (accumulated) VEI value for each volcanic year. This is
113 because one can expect a cumulative volcanic influence on NLCs in term of a
114 cumulative injection of water vapor, methane and fine dust for each volcanic year.

115

116 **3. Method of Analysis**

117 Multiple regression analysis (MRA) has been applied to the analyzed NLC
118 parameters:

119

$$120 \quad Y = C_0 + C_1 \cdot (t - 1968) + C_2 \cdot F_{Ly\alpha}(t - t_{lag2}) + C_3 \cdot VEI(t - t_{lag3}) \quad (1)$$

121

122 where Y is the yearly estimated NLC parameter (either the NLC occurrence number or
123 NLC brightness), C_0 is the regression constant, C_1 , C_2 and C_3 are the regression
124 coefficients characterizing the linear long-term trend (Value per year, V/yr), solar
125 activity term (Value per SFU, solar Ly- α flux units, 1 SFU is 10^{11} photons $s^{-1}cm^{-2}$) and
126 volcanic activity term (Value per VEI value); t_{lag2} and t_{lag3} are the phase time lags
127 between the NLC parameter and solar activity and volcanic activity, respectively, $F_{Ly\alpha}$
128 is the Lyman α flux averaged over each summer season (June-July), and VEI is the
129 total (accumulated) volcanic explosivity index for each volcanic year. The same MRA
130 technique has been frequently utilized in geophysical data analysis (Dalin et al., 2020;
131 DeLand et al., 2015; Dubietis et al., 2010; Kirkwood et al., 2008; Pertsev et al., 2014).

132 All statistical errors presented in the paper have been calculated using the least-
133 squares method (Jenkins & Watts, 1968). The number of observations (N value) is

134 equal to 51 for NLC, volcanic and solar time series. The degree of freedom is 47. We
135 calculate various statistical significance levels (either 90% $\sim 1.5\sigma$, or 95% $\sim 2\sigma$, or
136 99% $\sim 3\sigma$) for the estimated regression coefficients (C_0 , C_1 , C_2 and C_3) in order to
137 demonstrate as high statistical significance for a particular regression coefficient as
138 possible. The P values for the null hypothesis test have been calculated for each
139 regression coefficient as well. All statistical levels as well as P values are presented in
140 Table 1.

141

142 **4. Results**

143 **4.1. Overview of the analyzed data on volcanic activity and noctilucent clouds.**

144 The analyzed data on volcanic and NLC activity for the period of 1968-2018 are
145 shown in Fig. 1. In this research, we analyze volcanic activity represented by VEI
146 values on a logarithmic scale (not on a linear scale). The reason for this is as follows.
147 We assume that the main driver of volcanic eruptions on NLC activity is due to
148 erupted water vapor to the troposphere and stratosphere which slowly ascend to the
149 mesopause region (80-90 km) as will be considered in the Discussion. Unfortunately,
150 there are no available estimations of amounts and eruptive heights of injected water
151 vapor to the atmosphere after each volcanic eruption so far. Fortunately, in the
152 analyzed volcanic data base there are estimations of the mass and eruptive altitudes of
153 one of the main volcanic gas sulfur dioxide (SO_2). These estimations were made
154 based on satellite measurements for some small part of volcanic eruptions, i.e., for
155 about 15% of all analyzed volcanic eruptions for the past five decades. The eruptive
156 altitudes and masses of SO_2 as a function of VEI values are shown in Fig. 2 (panels a
157 and b, respectively). One can see that there are wide ranges of SO_2 altitudes and
158 masses for a given VEI value (black dots), that is especially valid for small and
159 moderate eruptions with VEI values from 1 to 3. At the same time, we can estimate
160 mean values of the altitudes and masses of SO_2 for each VEI value, which are shown
161 in Fig. 2 by red dots. A statistical F-test demonstrates that the mean values are well
162 described by the logarithmic function of VEI values (the blue lines in Fig. 2a and Fig.
163 2b have 96% and 88% significance, respectively). Since water vapor is one of the
164 main volcanic gases (Symonds et al., 1994), we can assume that masses and altitudes
165 of eruptive water vapor have the logarithmic dependence of VEI values as well.
166 Further we will consider NLC activity as a function of the sum of VEI values for each
167 year for the period of 1968-2018.

168

169 **4.2. Dependence of noctilucent cloud activity on volcanic activity.**

170 Since the phase time lag between NLC and volcanic activities (t_{lag3}) is completely
171 unknown so far, we have performed our analysis using t_{lag3} values in a wide range
172 from minus ten to plus ten years. The minus/ plus phase shift means that NLC activity
173 is ahead of/ follows volcanic one. All the calculated regression coefficients and time
174 lags of equation (1) are summarized in Table 1.

175 The calculated volcanic regression coefficient C_3 as a function of the time lag is
176 illustrated in Fig. 3a,c. We can see there is statistically significant (90%) positive
177 volcanic regression coefficient C_3 with the correlation lag equal to +7 years in the
178 case of the NLC occurrence number (Fig. 3a). The cross-correlation coefficient for
179 this peak value is +0.35 (Fig. 3b). At the same time, the cross-correlation coefficient
180 between NLC and solar activity is equal to -0.30 with the phase lag of zero years, i.e.,
181 less than the cross-correlation coefficient of volcanic activity. This finding clearly
182 illustrates a comparable and even dominating role of the volcanic forcing relative to
183 well-known anticorrelation solar influence leading to photodissociation of water
184 molecules at the mesopause region. The same analysis has been performed for the
185 NLC brightness. Figure 3c demonstrates us that there is statistically significant (90%)
186 positive influence of volcanic activity on the NLC brightness, with the same +7 years
187 phase shift as obtained for the NLC occurrence number. The cross-correlation
188 coefficient of this peak regression value is equal to +0.36 (Fig. 3d), again slightly
189 greater by absolute value than the cross-correlation coefficient of solar activity.

190 Now we consider the influence of volcanic activity on NLCs by selecting volcanic
191 eruptions which occurred at equatorial and subtropical latitudes between 30°S and
192 30°N . The reason for this is considered in the Discussion. One can see that for the
193 NLC occurrence number (Fig. 4a) the volcanic regression coefficient has now
194 increased from 0.11 to 0.15 at the 7-year time lag, and its statistical significance has
195 also become higher than 95%. A similar result has been obtained for the NLC
196 brightness (Fig. 4c), which shows statistically significant (95%) positive influence of
197 volcanic activity with the same phase shift of +7 years. The maximum cross-
198 correlation coefficients for the NLC occurrence number and brightness are +0.39 (Fig.
199 4b,d), i.e., greater than in case when considering all volcanic eruptions that occurred
200 around the world.

201 One can investigate a role of the power of volcanic eruptions influencing the NLC
202 activity. We can do it by selecting volcanic eruptions in accordance to their VEI
203 values. As in Fig. 4, all the eruptions have been considered in the latitude band
204 between 30°S and 30°N. The volcanic regression coefficients for minor volcanic
205 eruptions, having VEI values equal to 1 and 2 points, are shown for the NLC
206 occurrence number (Fig. 5a) and NLC brightness (Fig. 5c). One can see none of
207 volcanic regression coefficients (C_3) are statistically significant. At the same time, if
208 we consider moderate and large volcanic eruptions with VEI values equal to 3 points
209 and more, then the picture dramatically changes: highly statistically significant
210 volcanic influence (99%) is found for both the NLC occurrence number (Fig. 5b) and
211 NLC brightness (Fig. 5d), with the same phase lag equal to +7 years. Note that such a
212 high statistical significance of 99% in the NLC occurrence number and brightness is
213 rarely observed in actual geophysical data having large random errors due to the
214 presence of various processes. Nevertheless, the 99% statistical significance of the
215 volcanic driver on NLC activity does exist in the analyzed data sets.

216

217 **5. Discussion**

218 About zero long-term trend in the occurrence frequency of noctilucent clouds and
219 small positive statistically insignificant long-term trend in their brightness (see
220 coefficients C_7 in Table 1) have been obtained in the present study. It means that these
221 small trends are not reliable and they might readily change their signs in the years to
222 come. This result agrees with numerous ground-based NLC observations performed
223 around the world (Dalin et al., 2006, 2020; Dubietis et al., 2010; Kirkwood & Stebel,
224 2003; Kirkwood et al., 2008; Pertsev et al., 2014; Romejko et al., 2003; Zalcik et al.,
225 2016), which clearly demonstrated about zero and/or small positive statistically
226 insignificant trends in NLC occurrence number and brightness for the past five
227 decades.

228 The reason for the selection of volcanic eruption in relation to latitudes is as
229 follows. In the equatorial troposphere, there is an overturning wind circulation called
230 the Hadley Cells, in which the warm air rising at the equator sinks at around 30°S and
231 30°N latitudes where the Hadley Cells end (Brasseur & Solomon, 1986). However,
232 the Hadley Cells are not completely closed circulations. Part of the air penetrates into
233 the stratosphere in the tropics, then traveling towards polar latitudes of the summer
234 hemisphere, where it again rises to the summer mesosphere, and finally reaches the

235 summer mesopause (Brasseur & Solomon, 1986; Garcia & Solomon, 1983). This
236 meridional-vertical air circulation is supposed to be one of the main sources of water
237 vapor at the mesopause region to form NLC ice particles (Thomas, 1991). Another
238 important source of water vapor in the mesosphere is due to methane oxidation
239 (Brasseur & Solomon, 1986; Thomas, 1991). The photochemical lifetime of methane
240 in the troposphere, stratosphere and lower mesosphere is long enough (several years)
241 to produce sufficient amount of water vapor in the mesosphere and mesopause, i.e.,
242 one methane molecule produces about two molecules of water vapor (Thomas, 1991).
243 Our finding supports the penetration of volcanic gases (water vapor and methane)
244 from the troposphere through the tropical upwelling to the polar mesopause region by
245 highly statistically significant positive influence of volcanic activity on NLCs when
246 considering volcanic eruptions that occurred at the subtropics between 30°S and
247 30°N. Higher volcanic activity leads to higher positive influence on NLC activity that
248 is explained by larger amounts of volcanic gases injected to the tropical troposphere
249 and lower stratosphere, including water vapor and methane.

250 The found 7 years phase lag between volcanic and NLC activity is supported by
251 experimental studies dealing with the transport time of minor atmospheric species
252 from the troposphere to the stratosphere and mesosphere. Thus, the transport time of
253 inert trace gases (N₂O, CF₂C₁₂, CFC₁₃ and CC₁₄) from the ground to the
254 stratosphere (at 20-30 km altitude) have been observed to be of the order of 3-4 years
255 (Stordal et al., 1985). Russell III *et al.* (1996) have found that the transport time of
256 hydrogen fluoride (HF) trace gas is 5.9±2 years to be lifted from the lower
257 troposphere to the mesosphere at 55 km altitude. The transport time of the CO₂ trace
258 gas (as measured in a balloon-borne experiment) was found to be about 5 years to
259 reach the polar stratosphere at 35 km altitude from the troposphere through the
260 tropical upwelling (Bischof et al., 1985). Thus, it takes about 4-6 years for inert trace
261 gases to reach the polar atmosphere at 30-55 km altitude from the tropical
262 troposphere. Then it takes them two years more to rise throughout the mesosphere and
263 reaching the mesopause region at 85-87 km altitude where NLC ice particles start to
264 form. The latter is supported by a well know fact that first undoubtedly detected NLCs
265 were discovered in June 1885, i.e., about two years after the explosive Krakatoa
266 eruption occurred in August 1883. Note that the most likely altitude of the Krakatoa
267 eruption column was about 40–50 km (Carey & Sparks, 1986; Self & Rampino,

268 1981). As a result, the total time required transporting volcanic water vapor and
269 methane from the tropical troposphere to the polar mesopause is about 6-8 years. This
270 does not apply to the most violent volcanic eruptions, such as Krakatoa, El Chichón
271 and Pinatubo, in which volcanic plumes can be injected higher up into the middle and
272 upper stratosphere. Our finding of the 7 years time delay between NLCs and volcanic
273 activity is in a good agreement with the above mentioned experimental estimations.

274 Another potential volcanic mechanism influencing NLC activity is as follows.
275 Besides water vapor and methane, volcanic eruptions inject SO₂ into the stratosphere,
276 which leads to increased sulfate aerosol optical depth, which in turn warms the
277 stratosphere (Randel et al., 2009). Warming of the stratosphere results in warming of
278 the mesosphere and mesopause through hydrostatic atmospheric expansion (Akmaev
279 et al., 2006), which in turn should lead to a decrease in NLC activity, i.e., one can
280 anticipate an anticorrelation behavior between volcanoes and NLCs in this case.
281 However, by looking at the volcanic regression coefficient (C_3) as a function of time
282 lag shown in Figs. 3-5, we see that all negative volcanic regression coefficients are
283 less compared to the pronounced positive volcanic regression coefficient at the lag of
284 7 years, and all these negative volcanic regression coefficients have small or no
285 statistical significance at all. This does not necessarily exclude the presence of the
286 volcanic warming mechanism but compared to the injection and transport of water
287 vapor, the latter seems to play a more significant role in establishing the connection
288 between NLCs and volcanic activity.

289 The limitations of our statistical study are due to unknown amounts of injected
290 volcanic water vapor after each eruption, how much ejected water vapor are actually
291 transported through the stratosphere and mesosphere as well as how long does it
292 actually take to transport volcanic gases to mesopause heights after each eruption.
293 This task is complicated. Indeed, a model study by Pinto et al., 1989 has clearly
294 indicated that after major volcanic eruptions increased water vapor in the stratosphere
295 is limited by condensation in the rising volcanic plume and stabilized ash cloud (cold
296 trap effect). The authors have emphasized that “*Cold trap effects in volcanic eruption*
297 *columns could exert significant controls on the amounts of water vapor and halogens*
298 *that remain in stratospheric volcanic clouds, through condensation on ash particles*
299 *followed by the fallout of the particles. It is extremely difficult to estimate the amount*
300 *of HCl and H₂O remaining in the stratosphere after volcanic eruptions, based on*
301 *current data and modeling capabilities.*” At the same time, the results of our statistical

302 study (positive response of NLCs to volcanic activity with a 7 years phase lag) are
303 consistent with a general atmospheric meridional-vertical circulation of minor
304 atmospheric species from the tropical troposphere to the polar mesopause region. This
305 will further stimulate us to make a sophisticated research dealing with satellite
306 measurements of water vapors in relation to volcanic eruptions, estimating H₂O
307 transport through the troposphere, stratosphere and mesosphere, and finding a robust
308 link between erupted volcanic water vapor and activity of noctilucent clouds.

309

310 **6. Conclusions**

311 We have analyzed long-term data sets of noctilucent clouds, volcanic and solar
312 activity from 1968 to 2018 and conclude the following:

- 313 1. For the first time, we have quantitatively investigated a factor of volcanic activity
314 in variability of NLCs for the past five decades. Our analysis reveals that there is
315 statistically significant positive influence of volcanic activity on changes in NLC
316 activity, with a time lag of 7 years between these processes which might be
317 explained by a slow meridional-vertical updraft of ejected volcanic water vapor
318 from the tropical troposphere to the polar mesopause.
- 319 2. The strongest influence of volcanic activity on NLCs, with 99% statistical
320 significance, is found for volcanic eruptions that occurred at tropical latitudes
321 between 30°S and 30°N, with VEI values equal and more than 3.
- 322 3. We have confirmed our previous results on no statistically significant long-term
323 trend in NLC activity at middle and subpolar latitudes for the past five decades as
324 well as statistically significant negative response of NLCs to solar activity.

325

326 **Acknowledgements:** The authors are grateful to all amateur observers for their help
327 in visual observations of noctilucent clouds conducted in the Moscow region from
328 1962 to 2002. The work was partly supported by the Russian Foundation for Basic
329 Research under project 19-05-00358a. The analyzed data sets on noctilucent clouds,
330 solar and volcanic activity (on a yearly base) for the period of 1968-2018 is available
331 at the project web site:

332 http://ifaran.ru/lab/lfva/terrestrial_and_space_effects_in_NLC.html?&locale=en

333

334

335

336

337 **References**

338 Akmaev, R. A., Fomichev, V. I. & Zhu, X. (2006). Impact of middle-atmospheric
339 composition changes on greenhouse cooling in the upper atmosphere. *Journal of*
340 *Atmospheric and Solar-Terrestrial Physics*, 68, 1879–1889.

341 Berger, U. & Lübken, F.-J. (2015). Trends in mesospheric ice layers in the
342 Northern Hemisphere during 1961–2013. *Journal of Geophysical Research-*
343 *Atmospheres*, 120, 11277–11298.

344 Bischof, W., Borchers, R., Fabian, P. & Krüger, B. C. (1985). Increased
345 concentration and vertical distribution of carbon dioxide in the stratosphere. *Nature*,
346 316, 708-710.

347 Brasseur, G. & Solomon, S. (1986). *Aeronomy of the middle atmosphere*. Second
348 Edition, D. Reidel Publishing Company, Dordrecht, Holland.

349 Bronshten, V. A., & Grishin, N. I. (1970). *Noctilucent clouds*. Nauka, Moscow.

350 Carey, S. N. & Sparks, R. S. J. (1986). Quantitative models of fallout and
351 dispersal of tephra from volcanic eruption columns. *Bulletin of Volcanology*, 48, 109–
352 125.

353 Dalin, P., Kirkwood, S., Andersen, H., Hansen, O., Pertsev, N., Romejko, V.
354 (2006). Comparison of long-term Moscow and Danish NLC observations: statistical
355 results. *Annales Geophysicae*, 24, 2841-2849.

356 Dalin, P., Pertsev, N. & Romejko, V. (2012). Notes on historical aspects on the
357 earliest known observations of noctilucent clouds. *History of Geo- and Space*
358 *Sciences*, 3, 87–97.

359 Dalin, P., Perminov, V., Pertsev, N. & Romejko, V. (2020). Updated long-term
360 trends in mesopause temperature, airglow emissions, and noctilucent clouds. *Journal*
361 *of Geophysical Research-Atmospheres*, 125, e2019JD030814,
362 <https://doi.org/10.1029/2019JD030814>.

363 DeLand, M. T., Shettle, E. P., Thomas, G. E. & Olivero, J. J. (2006). A quarter-
364 century of satellite PMC observations. *Journal of Atmospheric and Solar-Terrestrial*
365 *Physics*, 68, 9–29.

366 DeLand, M. T., & Thomas, G. E. (2015). Updated PMC trends derived from
367 SBUV data. *Journal of Geophysical Research-Atmospheres*, 120, 2140-2166.

368 DeLand, M. T. & Thomas, G. E. (2019). Extending the SBUV polar mesospheric
369 cloud data record with the OMPS NP. *Atmospheric Chemistry and Physics*, 19, 7913–
370 7925.

371 Dubietis, A., Dalin, P., Balciunas, R. & Cernis, K. (2010). Observations of
372 noctilucent clouds from Lithuania. *Journal of Atmospheric and Solar-Terrestrial*
373 *Physics*, 72, 14-15, 1090-1099.

374 Etiopé, G. & Milkov, A. V. (2004). A new estimate of global methane flux from
375 onshore and shallow submarine mud volcanoes to the atmosphere. *Environmental*
376 *Geology*, 46, 997-1002.

377 Fiedler, J., Baumgarten, G., Berger, U. & Lübken, F.-J. (2017). Long-term
378 variations of noctilucent clouds at ALOMAR. *Journal of Atmospheric and Solar-*
379 *Terrestrial Physics*, 162, 79–89.

380 Fogle, B. & Haurwitz, B. (1973). Long term variations in Noctilucent cloud
381 activity and their possible cause. *Climatological Research*, 263–276, Bonner
382 Meteorologische Abhandlungen, Bonn, Germany.

383 Gadsden, M. (1997). The secular changes in noctilucent cloud occurrence: Study
384 of a 31-year sequence to clarify the causes. *Advances in Space Research*, 20(11),
385 2097–2100.

386 Gadsden, M. (1990). A secular change in noctilucent cloud occurrence. *Journal of*
387 *Atmospheric and Terrestrial Physics*, 52(4), 247-251.

388 Garcia, R. R. & Solomon, S. (1983). A numerical model of the zonally averaged
389 dynamical and chemical structure of the middle atmosphere. *Journal of Geophysical*
390 *Research*, 88(C2), 1379-1400.

391 Hervig, M. & Siskind, D. (2006). Decadal and inter-hemispheric variability in
392 polar mesospheric clouds, water vapor, and temperature. *Journal of Atmospheric and*
393 *Solar-Terrestrial Physics*, 68, 30–41.

394 Hervig, M. E., Berger, U. & Siskind, D. E. (2016). Decadal variability in PMCs
395 and implications for changing temperature and water vapor in the upper mesosphere.
396 *Journal of Geophysical Research-Atmospheres*, 121, 2383–2392.

397 Jenkins, G. M. & Watts, D. G. (1968). *Spectral analysis and its applications*.
398 Holden-Day, San Francisco.

399 Kirkwood, S. & Stebel, K. (2003). Influence of planetary waves on noctilucent
400 cloud occurrence over NW Europe. *Journal of Geophysical Research*, 108(D8), 8440,
401 doi: 10.1029/2002JD002356.

402 Kirkwood, S., Dalin, P. & Réchou, A. (2008). Noctilucent clouds observed from
403 the UK and Denmark—Trends and variations over 43 years. *Annales Geophysicae*,
404 26, 1243–1254.

405 Kärcher, B., Dörnbrack, A. & Sölch, I. (2014). Supersaturation variability and
406 cirrus ice crystal size distributions. *Journal of the Atmospheric Sciences*, 71, 2905-
407 2926.

408 Lübken, F.-J. & Berger, U. (2011). Latitudinal and interhemispheric variation of
409 stratospheric effects on mesospheric ice layer trends. *Journal of Geophysical*
410 *Research*, 116, D00P03, doi:10.1029/2010JD015258.

411 Lübken, F.-J., Berger, U. & Baumgarten, G. (2018). On the anthropogenic impact
412 on long-term evolution of noctilucent clouds. *Geophysical Research Letters*, 45,
413 6681–6689.

414 Newhall, C. G. & Self, S. (1982). The Volcanic Explosivity Index (VEI): an
415 estimate of explosive magnitude for historical volcanism. *Journal of Geophysical*
416 *Research*, 87, 1231–1238.

417 Pertsev, N., Dalin, P., Perminov, V., Romejko, V., Dubietis, A., Balčiūnas, R. et al.
418 (2014). Noctilucent clouds observed from the ground: sensitivity to mesospheric
419 parameters and long-term time series. *Earth, Planets and Space*, 66(98),
420 doi:10.1186/1880-5981-66-98.

421 Pinto, J. P., Turco, R. P. & Toon, O. B. (1989). Self-limiting physical and
422 chemical effects in volcanic eruption clouds. *Journal of Geophysical Research*,
423 94(D8), 11165-11174.

424 Randel, W. J., Shine, K. P., Austin, J., Barnett, J., Claud, C., Gillett, N. P. et al.
425 (2009). An update of observed stratospheric temperature trends. *Journal of*
426 *Geophysical Research*, 114, D02107, doi:10.1029/2008JD010421.

427 Romejko, V. A., Dalin, P. A. & Pertsev, N. N. (2003). Forty years of noctilucent
428 cloud observations near Moscow: database and simple statistics. *Journal of*
429 *Geophysical Research*, 108(D8), 8443, doi:10.1029/2002JD002364.

430 Russell III, J. M., Luo, M., Cicerone, R. J. & Deaver, L. E. (1996). Satellite
431 confirmation of the dominance of chlorofluorocarbons in the global stratospheric
432 chlorine budget. *Nature*, 379, 526–529.

433 Self, S. & Rampino, M. (1981). The 1883 eruption of Krakatau. *Nature*, 294, 699–
434 704.

435 Shettle, E. P., DeLand, M. T., Thomas, G. E. & Olivero, J. J. (2009). Long term
436 variations in the frequency of polar mesospheric clouds in the Northern Hemisphere
437 from SBUV. *Geophysical Research Letters*, 36, L02803, doi:10.1029/2008GL036048.

438 Siebert, L., Simkin, T. & Kimberly, P. (2010). *Volcanoes of the World*. Third
439 Edition, University of California Press, Los Angeles.

440 Sigurdsson, H., Carey, S., Mandeville, C. & Bronto, S. (1990). Krakatau volcano
441 expedition 1990. *Report to the National Geographic Society*, 37 pp..

442 Stordal, F., Isaksen, I. S. A. & Horntveth, K. (1985). A diabatic circulation two-
443 dimensional model with photochemistry: simulations of ozone and long-lived tracers
444 with surface sources. *Journal of Geophysical Research*, 90(D3), 5757-5776.

445 Symonds, R.B., Rose W. I., Bluth G. J. S., & Gerlach T. M. (1994). Volcanic gas
446 studies: methods, results, and applications, *Volatiles in Magmas: Reviews in*
447 *Mineralogy*. Mineralogical Society of America, Washington, D.C., Eds. Carroll, M.
448 R., & Holloway, J. R., 30. 1-66.

449 Thomas, G. E. (1984). Solar Mesosphere Explorer measurements of polar
450 mesospheric clouds (noctilucent clouds). *Journal of Atmospheric and Terrestrial*
451 *Physics*, 46(9), 819-824.

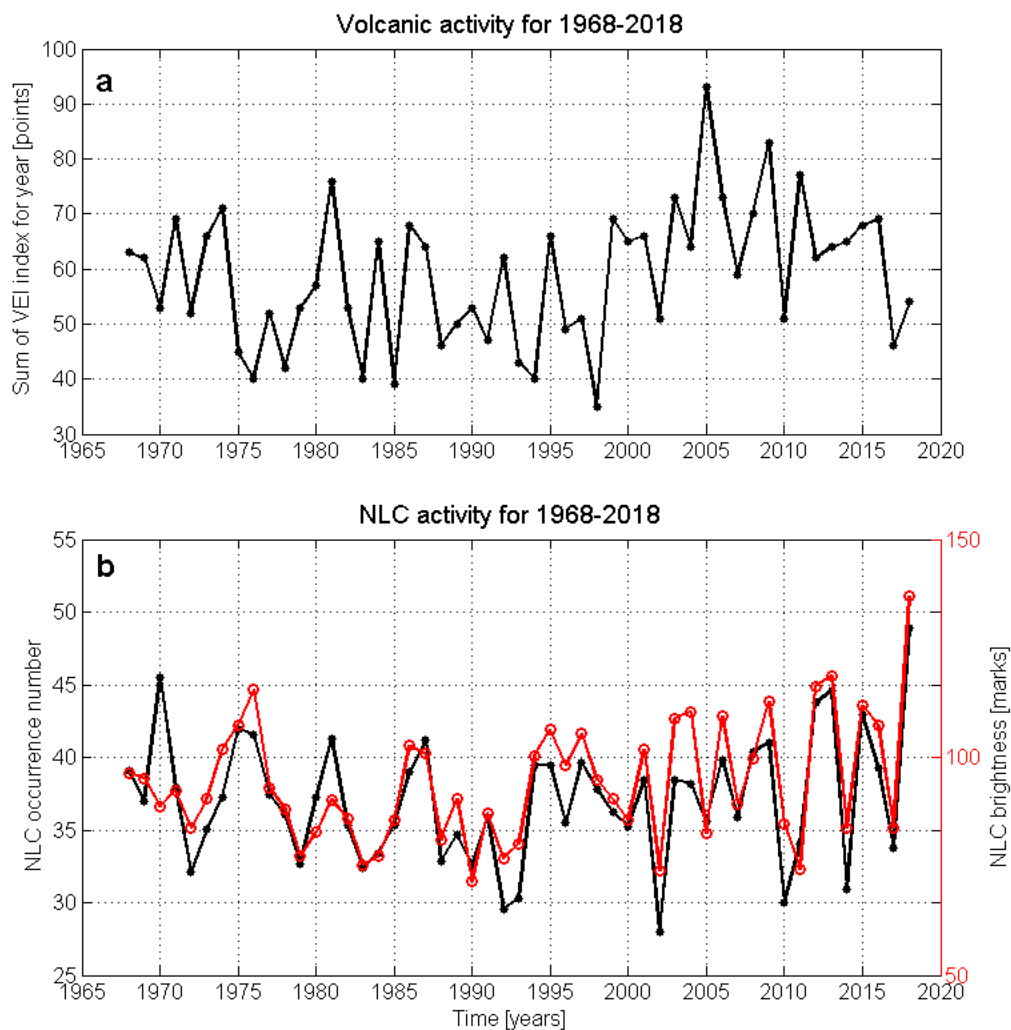
452 Thomas, G. E., Olivero, J. J., Jensen, E. J., Schroeder, W. & Toon, O. B. (1989).
453 Relation between increasing methane and the presence of ice clouds at the mesopause.
454 *Nature*, 338, 490–492.

455 Thomas, G. E. (1991). Mesospheric clouds and the physics of the mesopause
456 region. *Reviews of Geophysics*, 29(4), 553-575.

457 Thomas, G. E., and Olivero, J. (2001). Noctilucent clouds as possible indicators of
458 global changes in the mesosphere. *Advances in Space Research*, 28(7), 937-946.

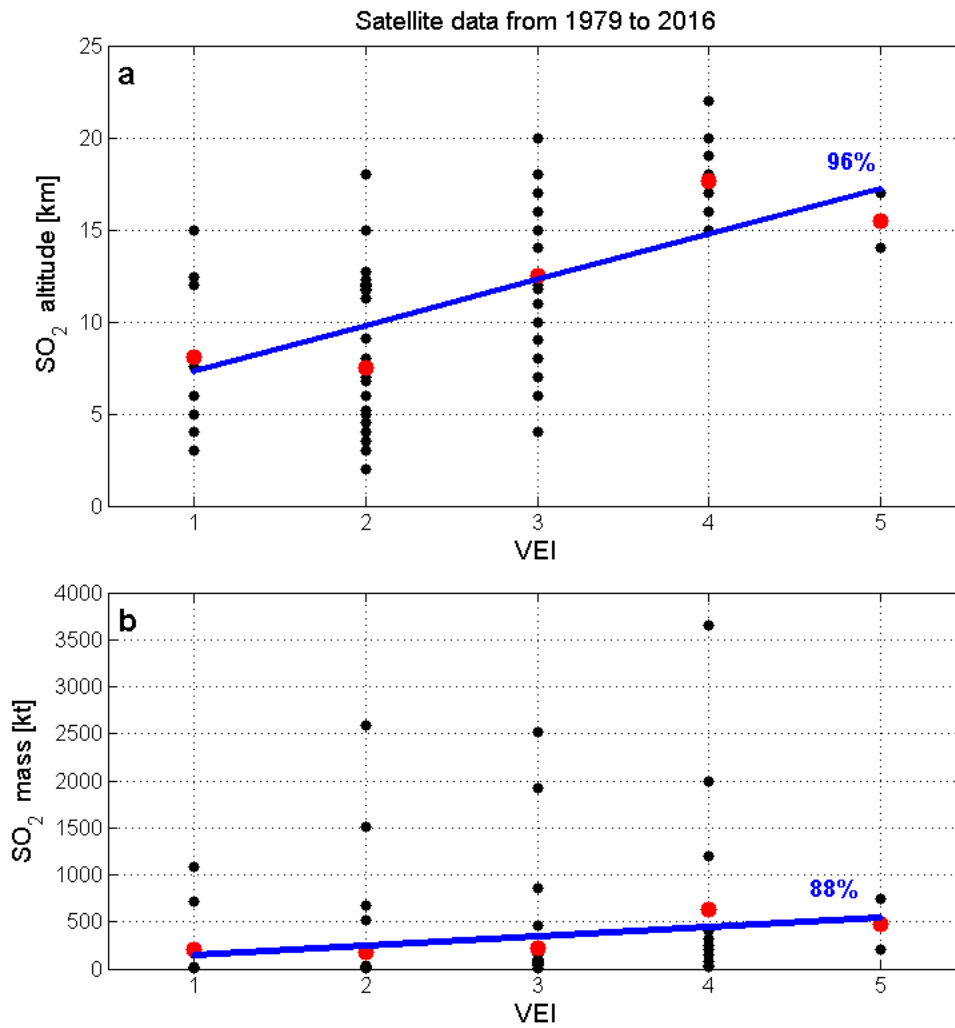
459 Zalcik, M. S., Lohvinenko, T. W., Dalin, P. & Denig, W. F. (2016). North
460 American noctilucent cloud observations in 1964-77 and 1988-2014: analysis and
461 comparisons. *Journal of the Royal Astronomical Society of Canada*, 110(1), 8-15.

462



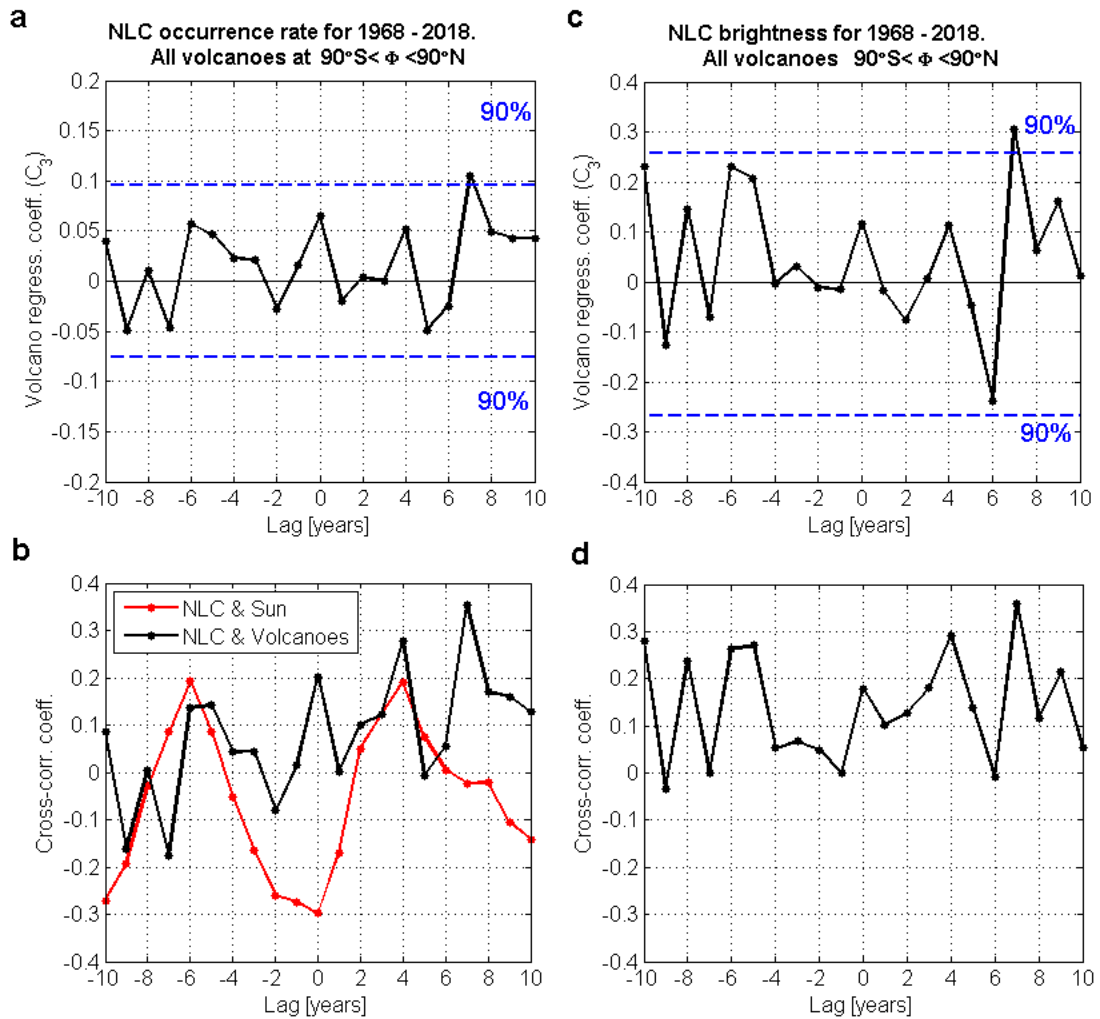
464

465 **Figure 1.** Overview of the analyzed data sets. (a) Volcanic activity data are
 466 represented by a sum of VEI values for each year from 1968 to 2018. Note that the
 467 two main eruptions in the time period considered (El Chichón in 1982 and Pinatubo in
 468 1991) do not show up in the annually accumulated VEI values. (b) Annual NLC
 469 activity for the period of 1968-2018 is represented by the annual NLC occurrence
 470 number (black line with dots, left Y axis) and by the annual NLC brightness (red line
 471 with open circles, right Y axis).



472

473 **Figure 2.** Satellite measurements of volcanic SO₂ emissions. (a) The black dots are
 474 eruptive altitudes of SO₂ emissions as a function of VEI values. The red dots are SO₂
 475 mean altitudes for the respective VEI values. The blue line is a linear function of
 476 mean SO₂ altitudes fitted in the least-square sense. (b) Same as in (a) except for the
 477 mass of ejected SO₂ emissions. Note that the X axis represents a logarithmic scale of
 478 the volcanic activity (VEI values). Linear regression functions are statistically
 479 significant with probabilities of 96% (a) and 88% (b).



480

481 **Figure 3.** Statistical quantities characterizing a connection between volcanic and NLC

482 activity for all volcanic eruptions that occurred around the world. (a) The black line

483 shows the volcanic regression coefficient (C_3) as a function of the phase time lag for

484 the NLC occurrence number. The blue lines indicate 90% confidence intervals of the

485 maximum value of the C_3 coefficient. (b) The black line shows the cross-correlation

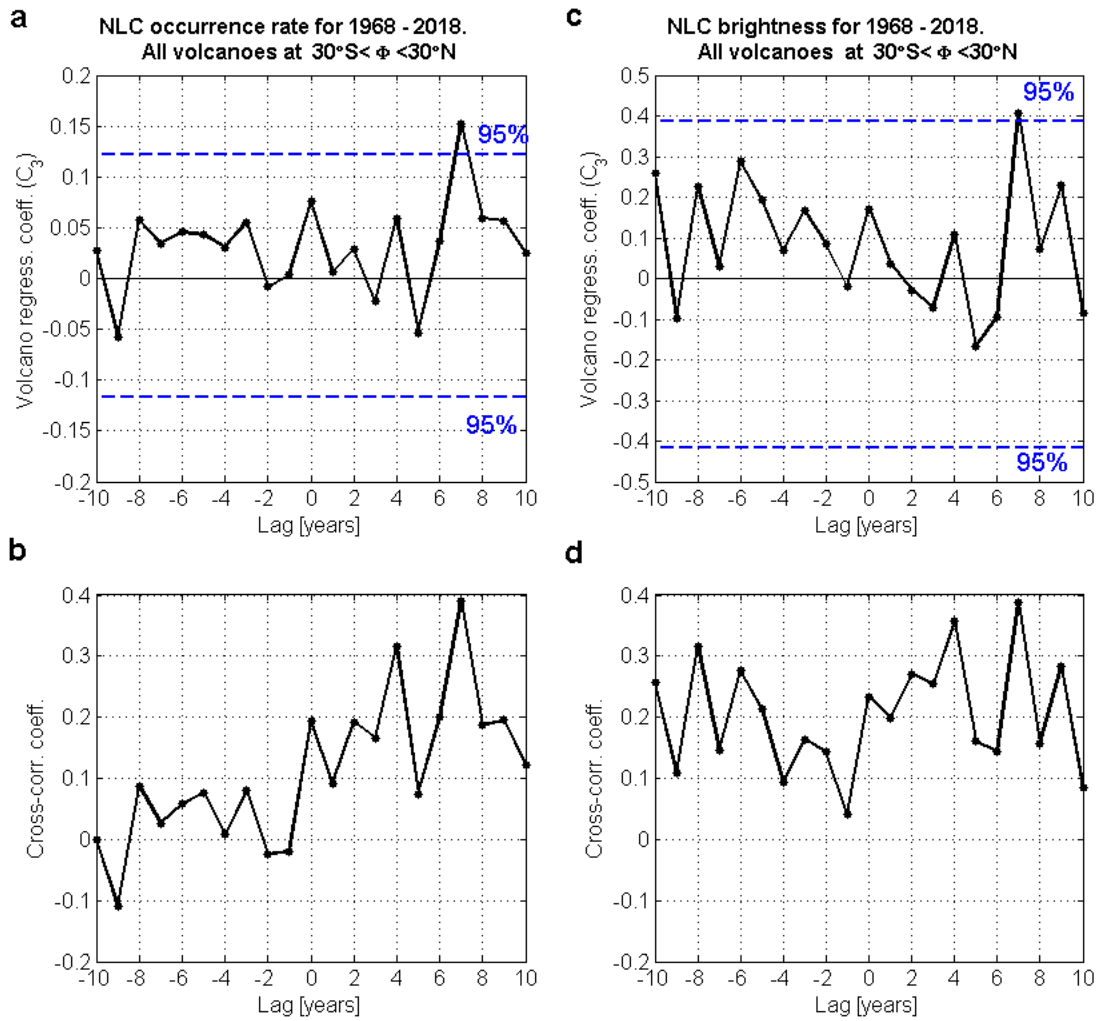
486 coefficient between the NLC occurrence number and volcanic activity. The red line

487 represents the cross-correlation coefficient between the NLC occurrence number and

488 solar Lyman α flux. (c) Same as in (a) except for the NLC brightness. (d) The black

489 line shows the cross-correlation coefficient between the NLC brightness and volcanic

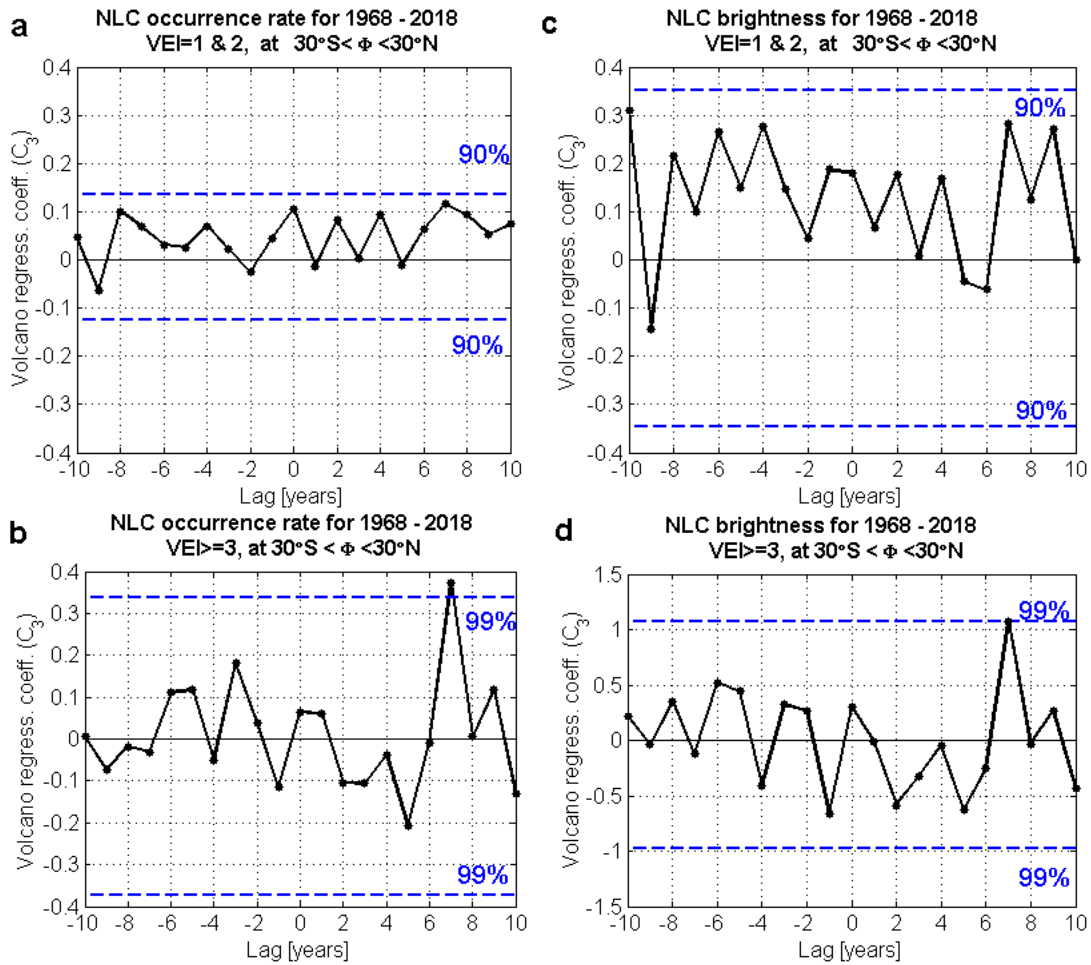
490 activity.



491
492

493 **Figure 4.** Statistical quantities characterizing a connection between volcanic and NLC
494 activity for all volcanic eruptions that occurred between 30°S and 30°N . (a) The back
495 line shows the volcanic regression coefficient (C_3) as a function of the phase time lag
496 for the NLC occurrence number. The blue lines indicate 95% confidence intervals of
497 the maximum value of the C_3 coefficient. (b) The cross-correlation coefficient is
498 between the NLC occurrence number and volcanic activity. (c) Same as in (a) except
499 for the NLC brightness. (d) Same as in (b) except for the NLC brightness.

500



501

502 **Figure 5.** Statistical quantities characterizing a connection between volcanic and NLC

503 activity for small, moderate and large volcanic eruptions that occurred between 30°S

504 and 30°N . **(a)** The black line shows the volcanic regression coefficient (C_3) for the

505 NLC occurrence number as a function of the phase time lag. The blue lines indicate

506 confidence intervals of the maximum value of the C_3 coefficient. Results for minor

507 volcanic eruptions, having VEI values equal to 1 and 2 marks, are shown. **(b)** Same as

508 in **(a)** for moderate and large volcanic eruptions, having VEI values equal to 3 and

509 more points. **(c)** Same as in **(a)** except for the NLC brightness. **(d)** Same as in **(b)**

510 except for the NLC brightness.

511

512 **Figure Legends**

513 **Figure 1.** Overview of the analyzed data sets. **(a)** Volcanic activity data are
514 represented by a sum of VEI values for each year from 1968 to 2018. Note that the
515 two main eruptions in the time period considered (El Chichón in 1982 and Pinatubo in
516 1991) do not show up in the annually accumulated VEI values. **(b)** Annual NLC
517 activity for the period of 1968-2018 is represented by the annual NLC occurrence
518 number (black line with dots, left Y axis) and by the annual NLC brightness (red line
519 with open circles, right Y axis).

520

521 **Figure 2.** Satellite measurements of volcanic SO₂ emissions. **(a)** The black dots are
522 eruptive altitudes of SO₂ emissions as a function of VEI values. The red dots are SO₂
523 mean altitudes for the respective VEI values. The blue line is a linear function of
524 mean SO₂ altitudes fitted in the least-square sense. **(b)** Same as in **(a)** except for the
525 mass of ejected SO₂ emissions. Note that the X axis represents a logarithmic scale of
526 the volcanic activity (VEI values). Linear regression functions are statistically
527 significant with probabilities of 96% **(a)** and 88% **(b)**.

528

529 **Figure 3.** Statistical quantities characterizing a connection between volcanic and NLC
530 activity for all volcanic eruptions that occurred around the world. **(a)** The black line
531 shows the volcanic regression coefficient (C_3) as a function of the phase time lag for
532 the NLC occurrence number. The blue lines indicate 90% confidence intervals of the
533 maximum value of the C_3 coefficient. **(b)** The black line shows the cross-correlation
534 coefficient between the NLC occurrence number and volcanic activity. The red line
535 represents the cross-correlation coefficient between the NLC occurrence number and
536 solar Lyman α flux. **(c)** Same as in **(a)** except for the NLC brightness. **(d)** The black
537 line shows the cross-correlation coefficient between the NLC brightness and volcanic
538 activity.

539

540 **Figure 4.** Statistical quantities characterizing a connection between volcanic and NLC
541 activity for all volcanic eruptions that occurred between 30°S and 30°N. **(a)** The black
542 line shows the volcanic regression coefficient (C_3) as a function of the phase time lag
543 for the NLC occurrence number. The blue lines indicate 95% confidence intervals of
544 the maximum value of the C_3 coefficient. **(b)** The cross-correlation coefficient is

545 between the NLC occurrence number and volcanic activity. **(c)** Same as in **(a)** except
546 for the NLC brightness. **(d)** Same as in **(b)** except for the NLC brightness.

547

548 **Figure 5.** Statistical quantities characterizing a connection between volcanic and NLC
549 activity for small, moderate and large volcanic eruptions that occurred between 30°S
550 and 30°N. **(a)** The black line shows the volcanic regression coefficient (C_3) for the
551 NLC occurrence number as a function of the phase time lag. The blue lines indicate
552 confidence intervals of the maximum value of the C_3 coefficient. Results for minor
553 volcanic eruptions, having VEI values equal to 1 and 2 marks, are shown. **(b)** Same as
554 in **(a)** for moderate and large volcanic eruptions, having VEI values equal to 3 and
555 more points. **(c)** Same as in **(a)** except for the NLC brightness. **(d)** Same as in **(b)**
556 except for the NLC brightness.

557

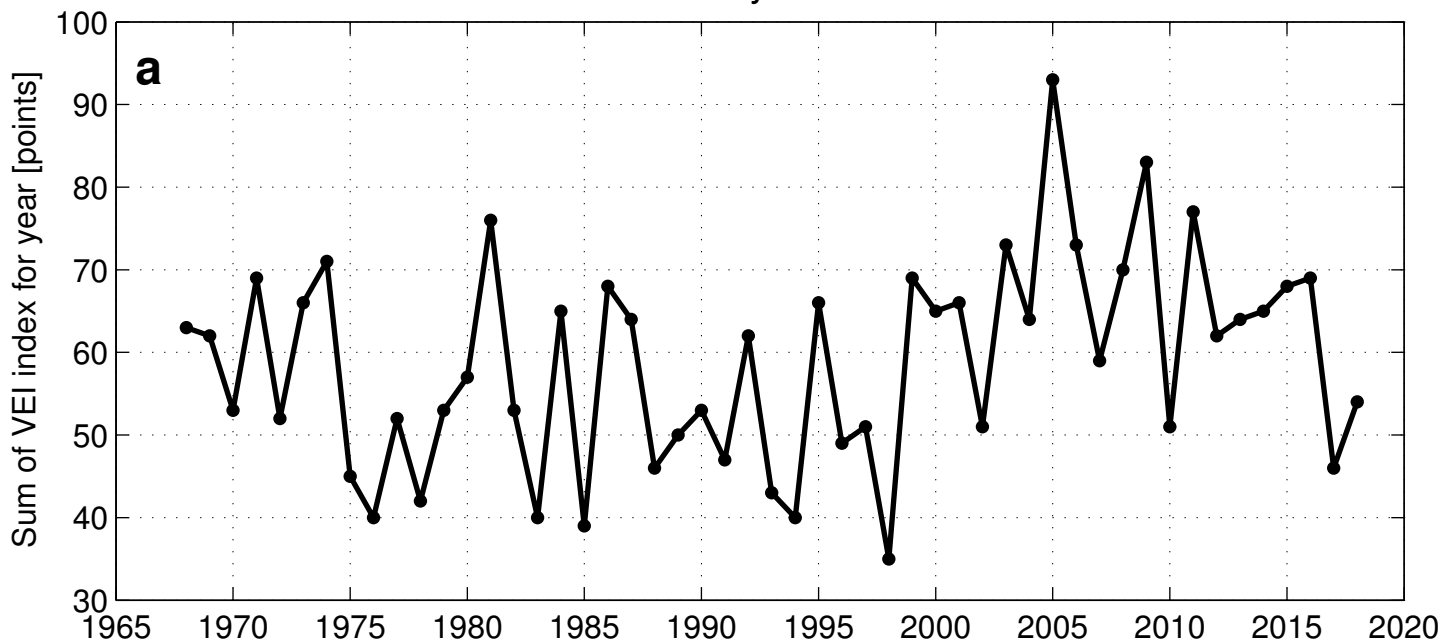
558 **Table 1.** Regression coefficients of the multiple regression model (see equation 1), along
559 with their standard deviations (1.5 or 2 or 3 standard deviations) for the NLC occurrence
560 number and NLC brightness for the period of 1968-2018. Corresponding confidence
561 probabilities (90% or 95% or 99%) are shown in brackets. Statistically significant
562 coefficients (equal to or greater than its error) at the corresponding confidence levels are
563 marked in bold. The time regression coefficient (C_1) is expressed in value per year (V/yr), the
564 solar regression coefficient (C_2) is expressed in value per solar flux unit (SFU, 10^{11} photons
565 $\text{cm}^{-2} \text{s}^{-1}$), the volcanic regression coefficient (C_3) is expressed in value per VEI (Value/VEI),
566 C_0 is the regression constant. Phase lags (years) are introduced for the Lyman α flux and VEI.
567 The P values for the null hypothesis test have been calculated for each regression coefficient.
568 Table 1 represents three model runs with three different selections of volcanic activity:
569 **a)** all volcanic eruptions that occurred around the world (all VEI values, all longitudes and all
570 latitudes);
571 **b)** volcanic eruptions with all VEI values at all longitudes and at latitudes between 30°S and
572 30°N;
573 **c)** volcanic eruptions with $\text{VEI} \geq 3$ at all longitudes and at latitudes between 30°S and 30°N.
574

(a) All volcanic eruptions (all VEI, all longitudes and all latitudes)				
	C_0 (V)	C_1 (V/yr)	C_2 (V/SFU) and lag (yr)	C_3 (V/VEI) and lag (yr)
NLC occurrence number	40.0±14.1 (99%), P=0.0	-0.003±0.087 (90%), P=0.960	-2.066±1.831 (95%), lag=0, P=0.028	0.105±0.083 (90%), lag=7, P=0.038
NLC brightness	111.1±44.3 (99%), P=0.0	0.159±0.272 (90%), P=0.330	-8.599±7.673 (99%), lag=0, P=0.004	0.305±0.259 (90%), lag=7, P=0.054
(b) Volcanoes with all VEI, all longitudes and latitudes between 30°S and 30°N				
NLC occurrence number	41.8±12.6 (99%), P=0.0	-0.027±0.089 (90%), P=0.619	-2.145±1.793 (95%), lag=0, P=0.020	0.152±0.122 (95%), lag=7, P=0.016
NLC brightness	117.3±39.9 (99%), P=0.0	0.102±0.284 (90%), P=0.549	-8.832±7.615 (99%), lag=0, P=0.003	0.406±0.387 (95%), lag=7, P=0.040
(c) Volcanoes with $\text{VEI} \geq 3$, all longitudes and latitudes between 30°S and 30°N				
NLC occurrence number	44.7±11.5 (99%), P=0.0	-0.021±0.084 (90%), P=0.674	-2.359±2.345 (99%), lag=0, P=0.010	0.373±0.339 (99%), lag=7, P=0.005
NLC brightness	124.8±36.4 (99%), P=0.0	0.106±0.267 (90%), P=0.506	-9.442±7.409 (99%), lag=0, P=0.001	1.070±1.071 (99%), lag=7, P=0.010

575

Figure 1.

Volcanic activity for 1968–2018



NLC activity for 1968–2018

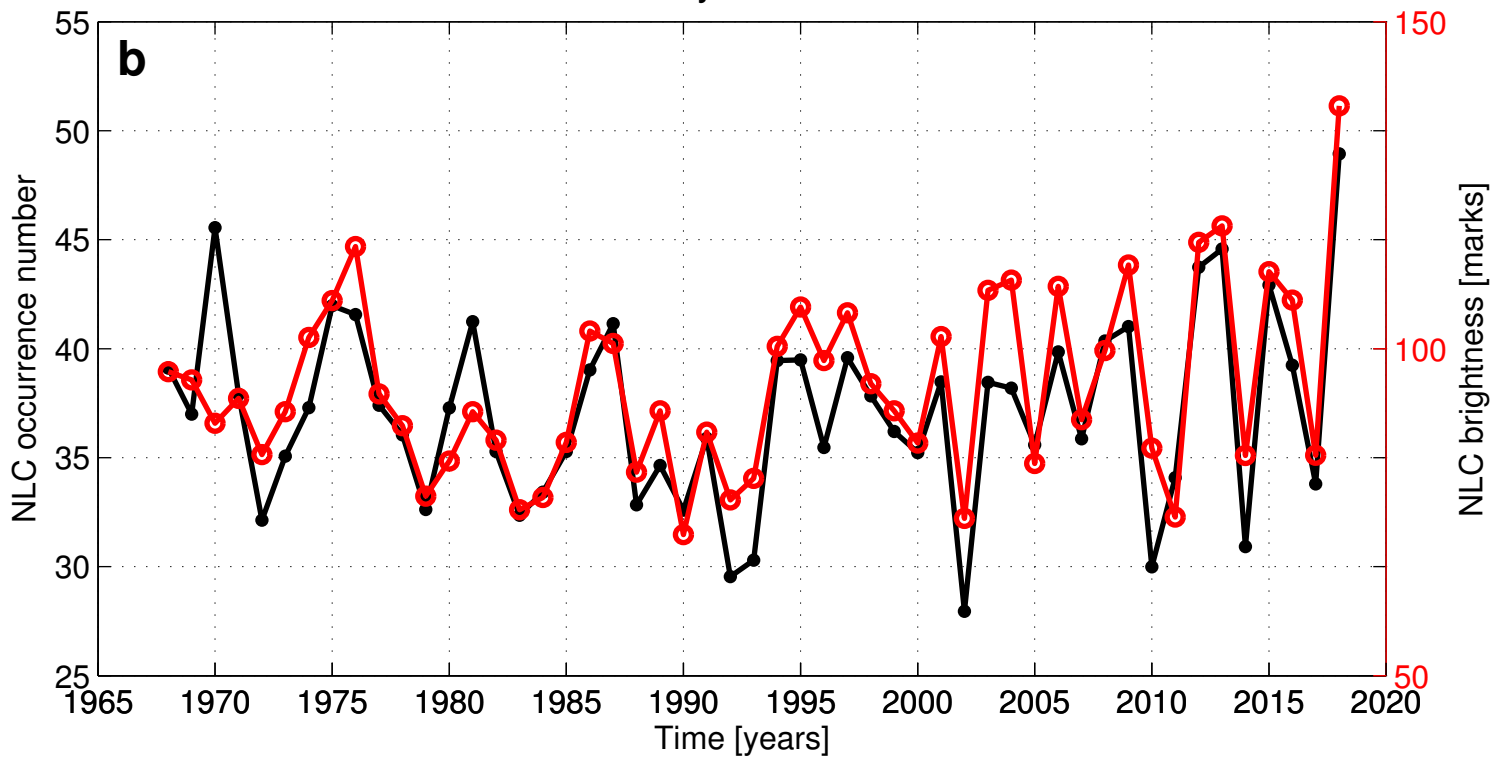


Figure 2.

Satellite data from 1979 to 2016

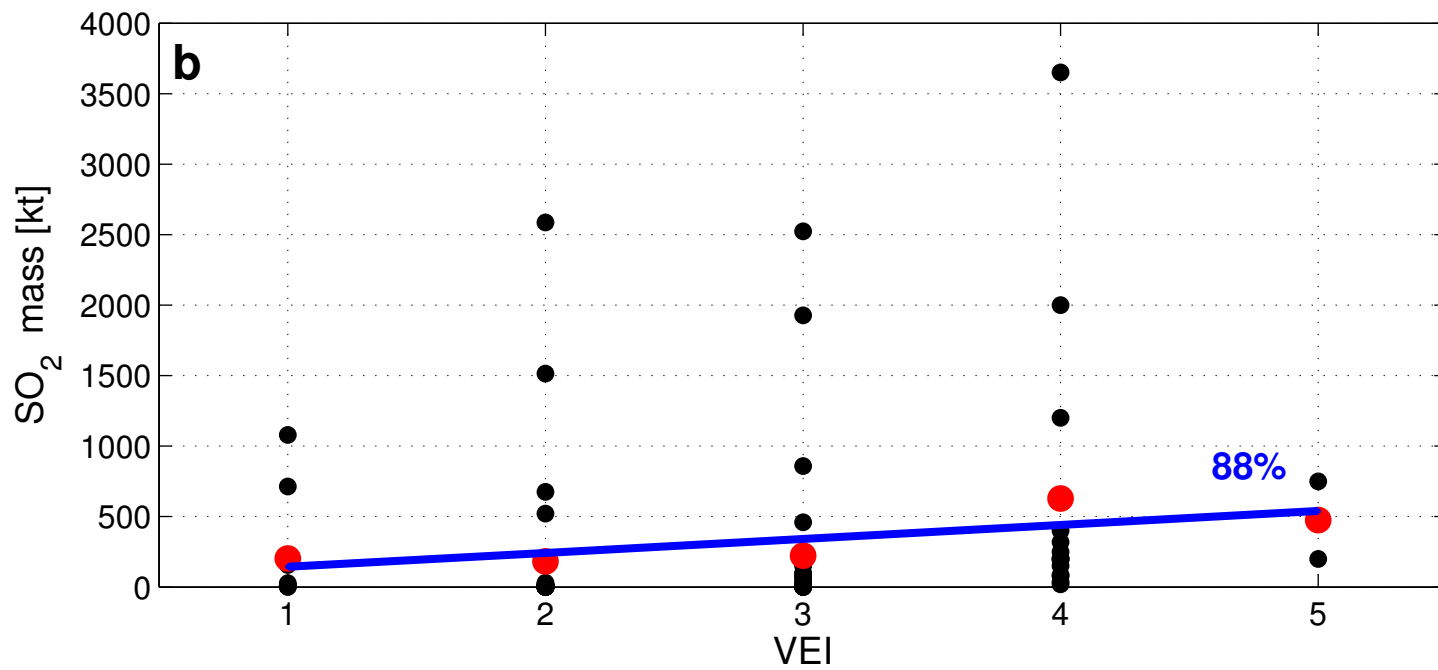
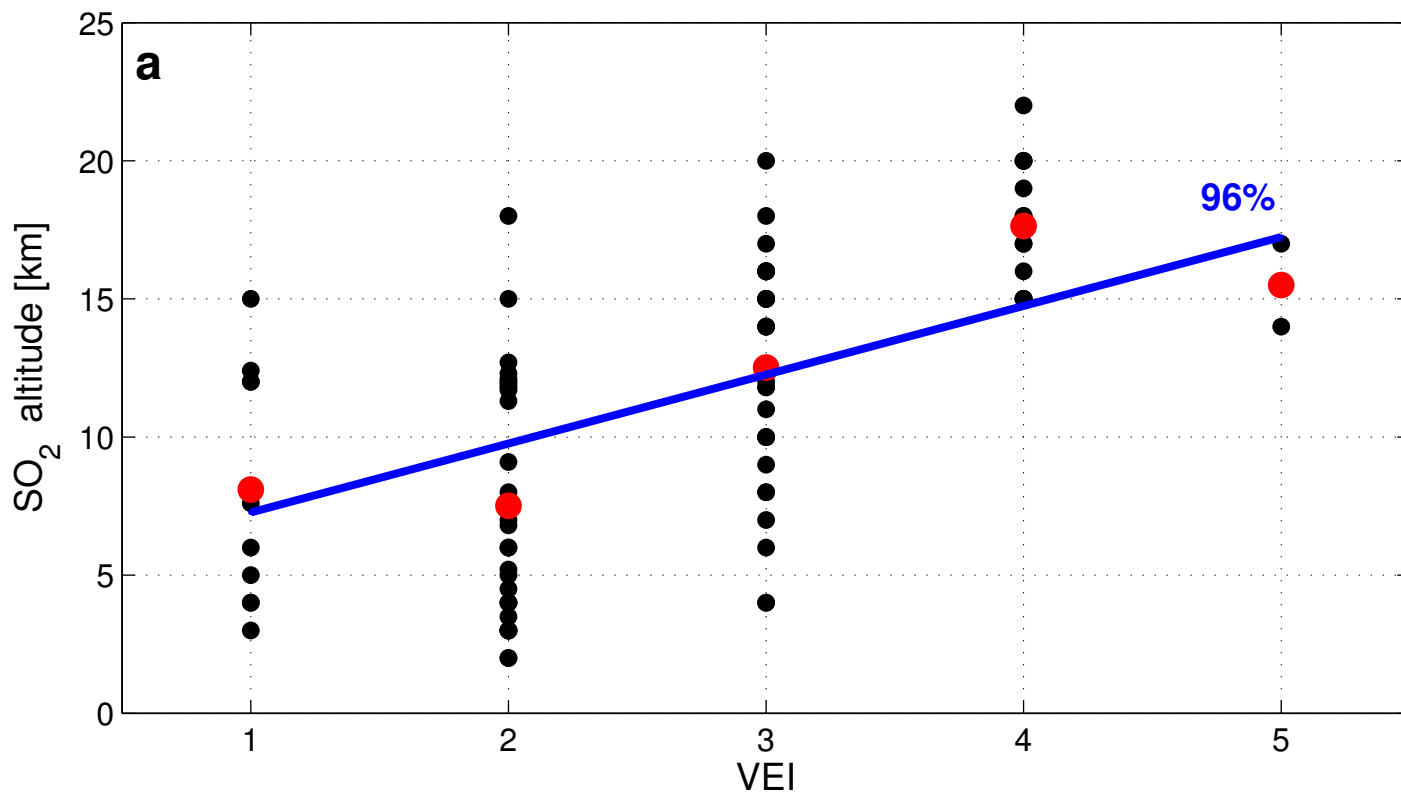
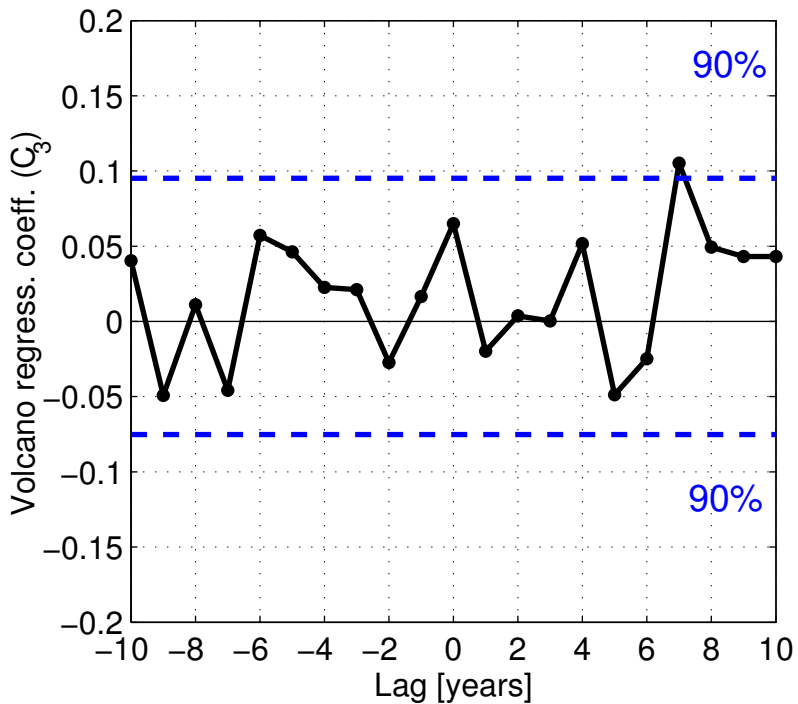
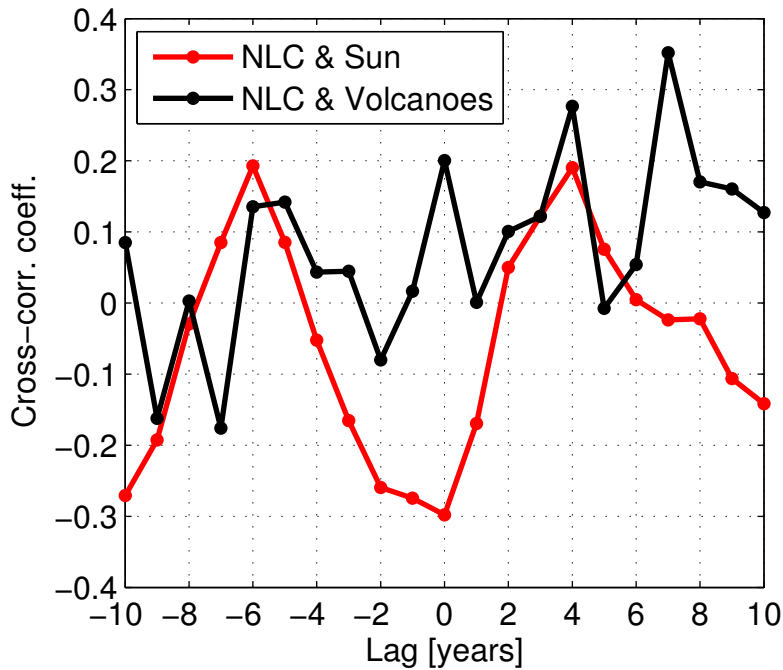


Figure 3.

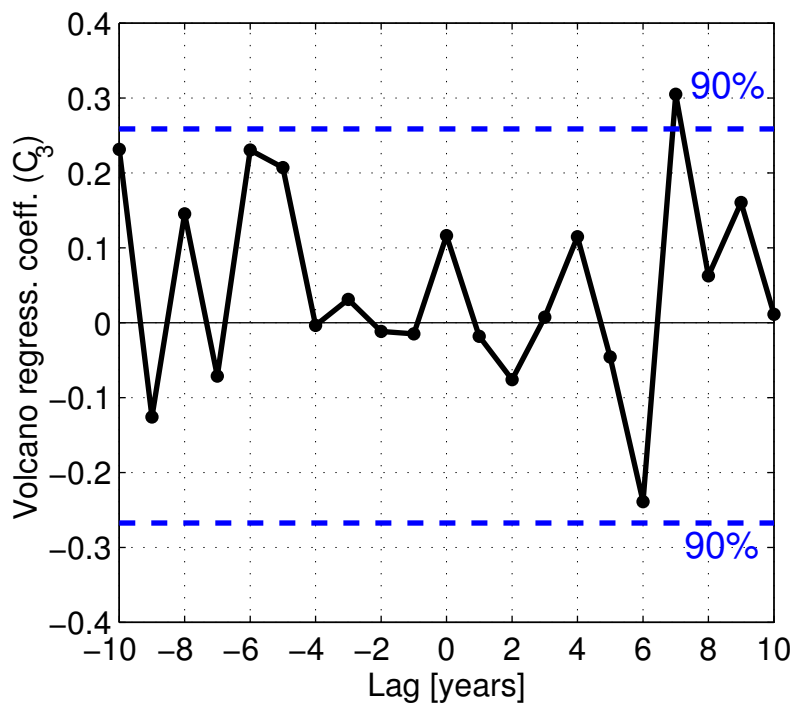
a NLC occurrence rate for 1968 – 2018.
All volcanoes at $90^{\circ}\text{S} < \Phi < 90^{\circ}\text{N}$



b



c NLC brightness for 1968 – 2018.
All volcanoes $90^{\circ}\text{S} < \Phi < 90^{\circ}\text{N}$



d

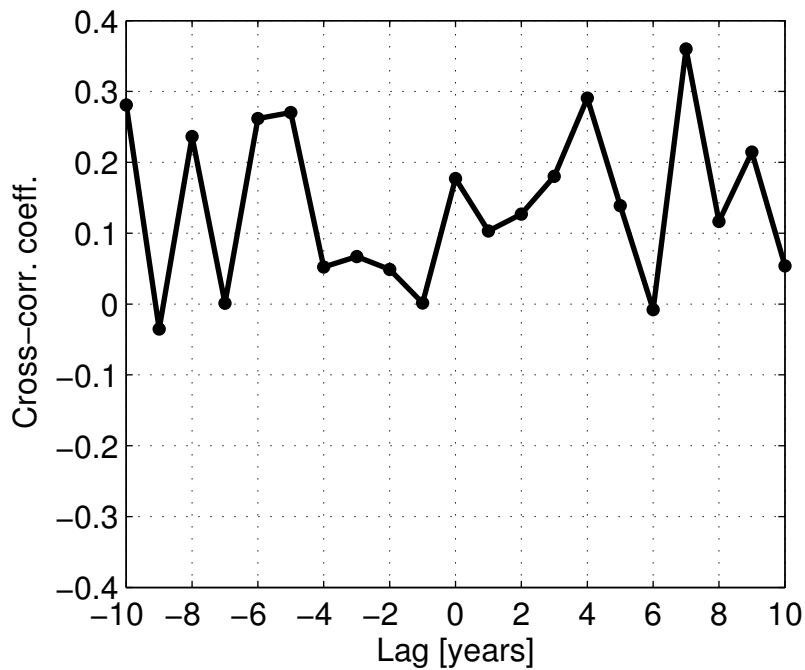
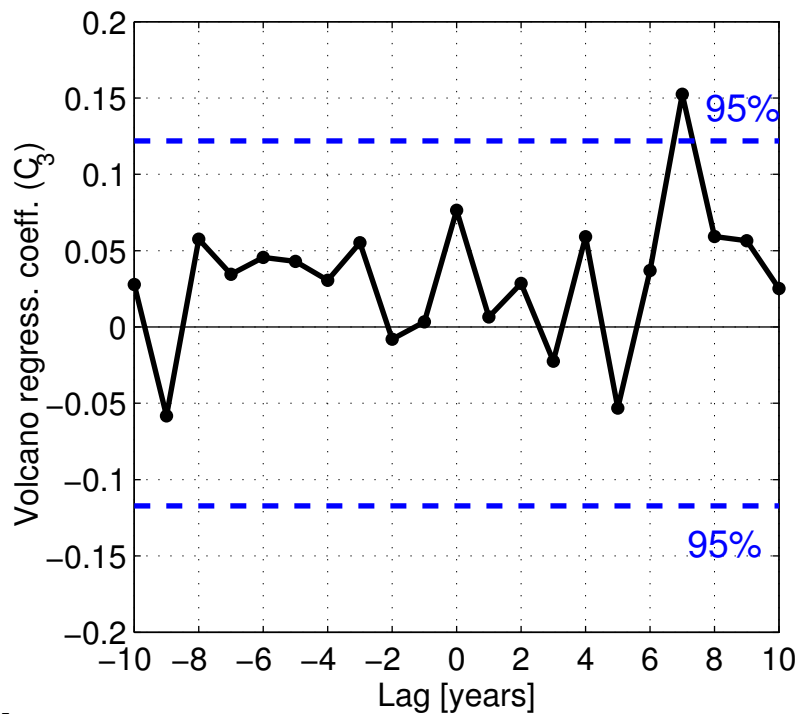


Figure 4.

a NLC occurrence rate for 1968 – 2018.
All volcanoes at $30^{\circ}\text{S} < \Phi < 30^{\circ}\text{N}$



c NLC brightness for 1968 – 2018.
All volcanoes at $30^{\circ}\text{S} < \Phi < 30^{\circ}\text{N}$

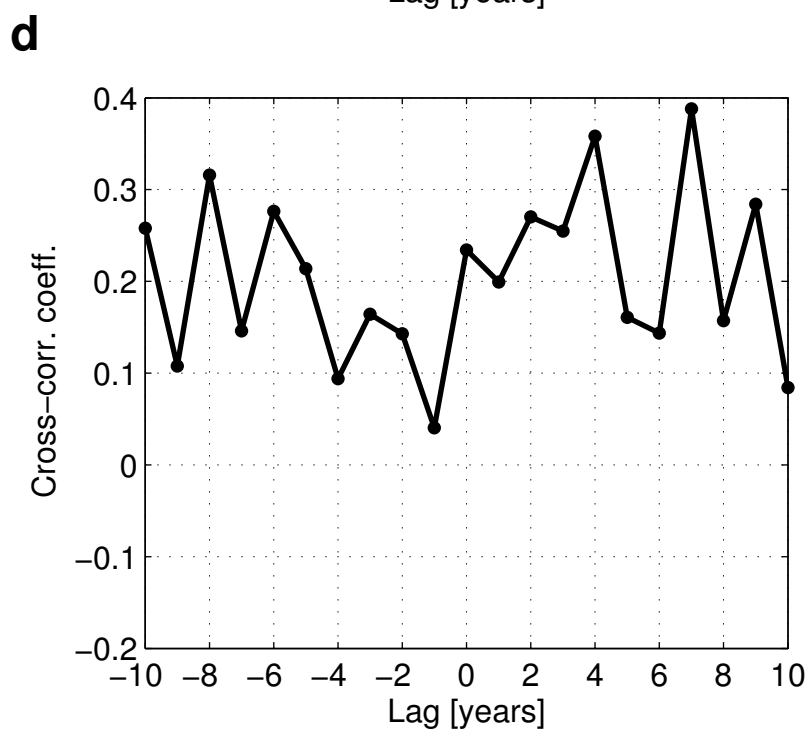
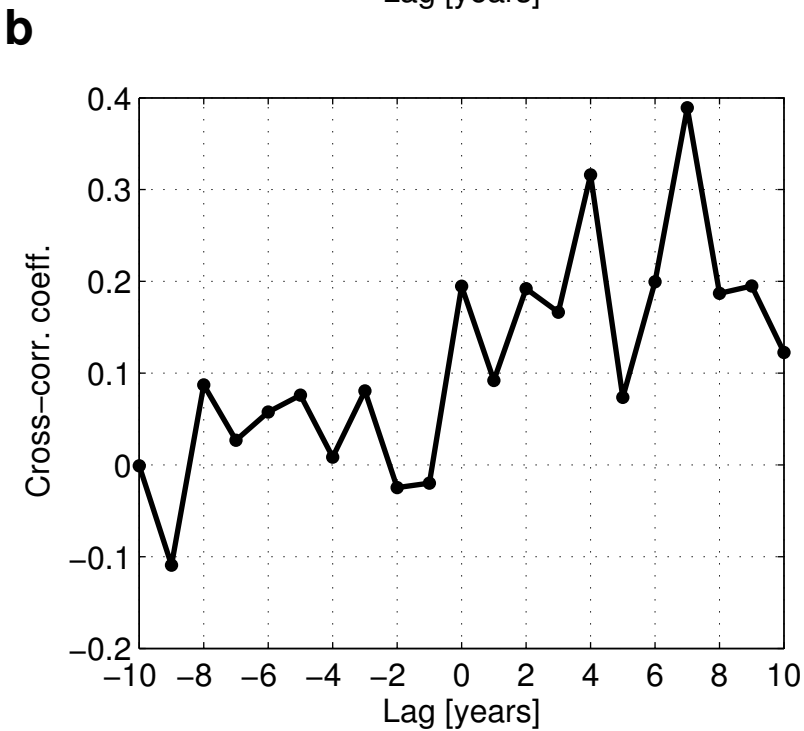
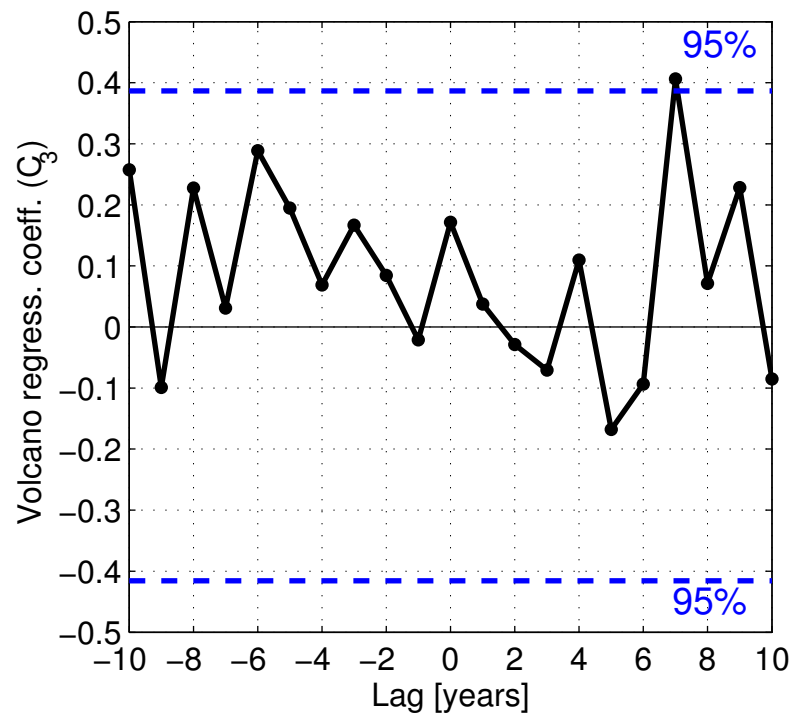
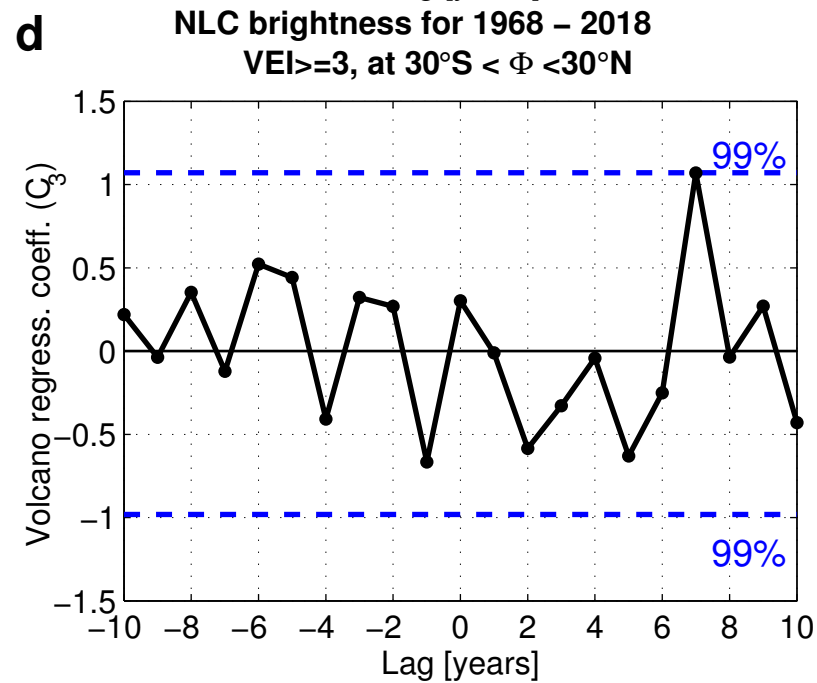
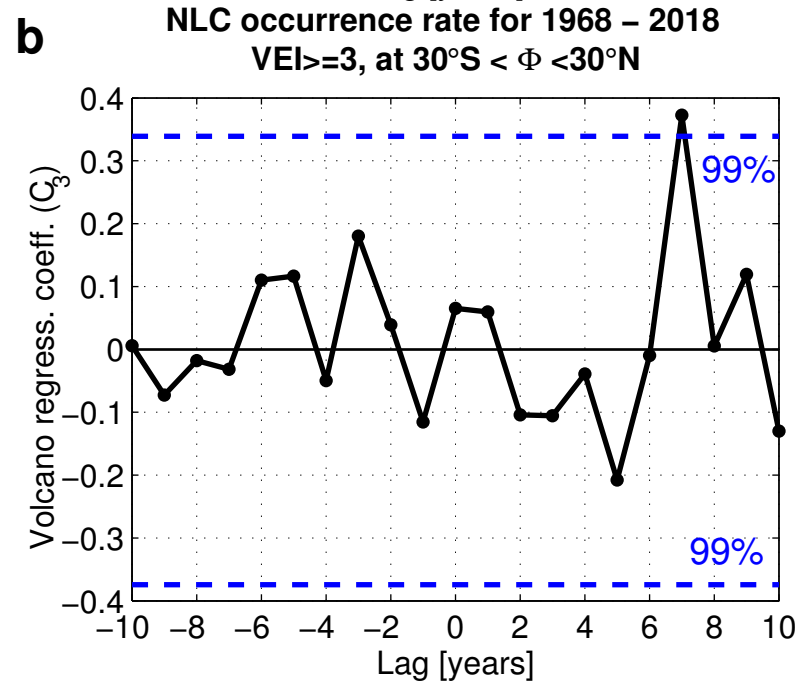
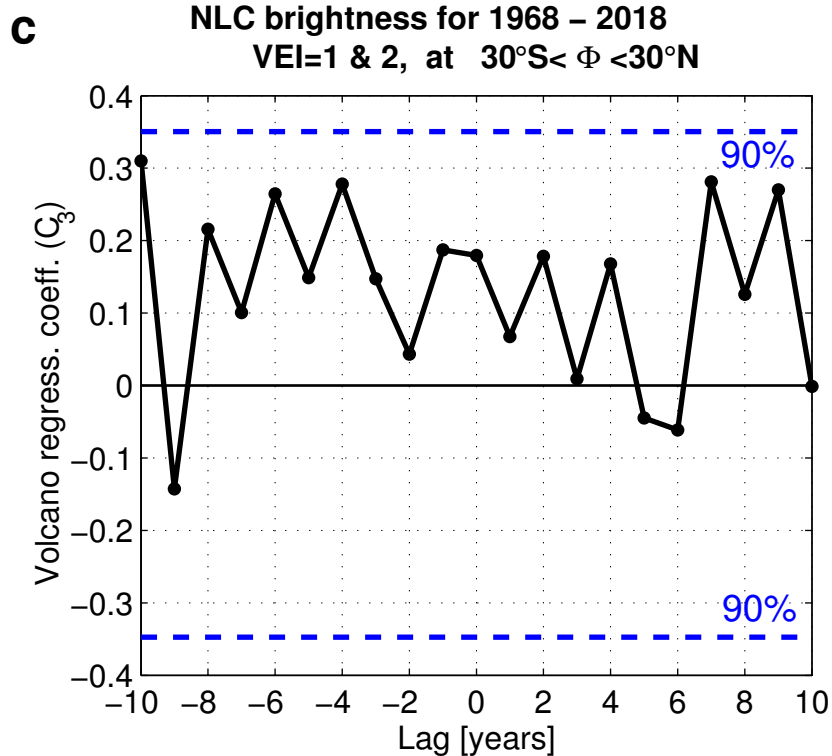
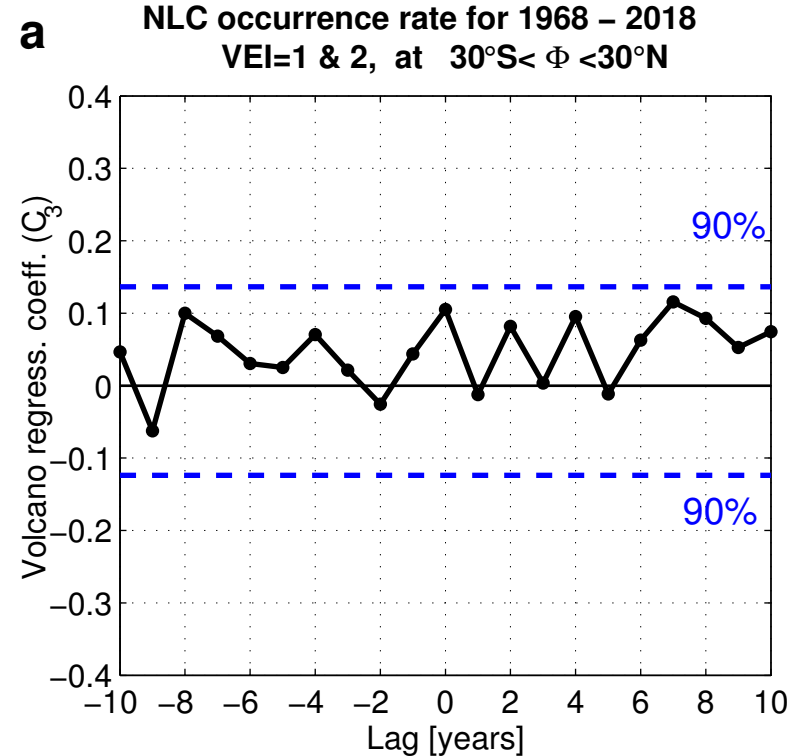


Figure 5.



1 **Table 1.** Regression coefficients of the multiple regression model (see equation 1), along
2 with their standard deviations (1.5 or 2 or 3 standard deviations) for the NLC occurrence
3 number and NLC brightness for the period of 1968-2018. Corresponding confidence
4 probabilities (90% or 95% or 99%) are shown in brackets. Statistically significant
5 coefficients (equal to or greater than its error) at the corresponding confidence levels are
6 marked in bold. The time regression coefficient (C_1) is expressed in value per year (V/yr), the
7 solar regression coefficient (C_2) is expressed in value per solar flux unit (SFU, 10^{11} photons
8 $\text{cm}^{-2} \text{s}^{-1}$), the volcanic regression coefficient (C_3) is expressed in value per VEI (Value/VEI),
9 C_0 is the regression constant. Phase lags (years) are introduced for the Lyman α flux and VEI.
10 The P values for the null hypothesis test have been calculated for each regression coefficient.
11 Table 1 represents three model runs with three different selections of volcanic activity:
12 **a)** all volcanic eruptions that occurred around the world (all VEI values, all longitudes and all
13 latitudes);
14 **b)** volcanic eruptions with all VEI values at all longitudes and at latitudes between 30°S and
15 30°N;
16 **c)** volcanic eruptions with VEI \geq 3 at all longitudes and at latitudes between 30°S and 30°N.
17

(a) All volcanic eruptions (all VEI, all longitudes and all latitudes)				
	C_0 (V)	C_1 (V/yr)	C_2 (V/SFU) and lag (yr)	C_3 (V/VEI) and lag (yr)
NLC occurrence number	40.0\pm14.1 (99%), P=0.0	-0.003 \pm 0.087 (90%), P=0.960	-2.066\pm1.831 (95%), lag=0, P=0.028	0.105\pm0.083 (90%), lag=7, P=0.038
NLC brightness	111.1\pm44.3 (99%), P=0.0	0.159 \pm 0.272 (90%), P=0.330	-8.599\pm7.673 (99%), lag=0, P=0.004	0.305\pm0.259 (90%), lag=7, P=0.054
(b) Volcanoes with all VEI, all longitudes and latitudes between 30°S and 30°N				
NLC occurrence number	41.8\pm12.6 (99%), P=0.0	-0.027 \pm 0.089 (90%), P=0.619	-2.145\pm1.793 (95%), lag=0, P=0.020	0.152\pm0.122 (95%), lag=7, P=0.016
NLC brightness	117.3\pm39.9 (99%), P=0.0	0.102 \pm 0.284 (90%), P=0.549	-8.832\pm7.615 (99%), lag=0, P=0.003	0.406\pm0.387 (95%), lag=7, P=0.040
(c) Volcanoes with VEI\geq3, all longitudes and latitudes between 30°S and 30°N				
NLC occurrence number	44.7\pm11.5 (99%), P=0.0	-0.021 \pm 0.084 (90%), P=0.674	-2.359\pm2.345 (99%), lag=0, P=0.010	0.373\pm0.339 (99%), lag=7, P=0.005
NLC brightness	124.8\pm36.4 (99%), P=0.0	0.106 \pm 0.267 (90%), P=0.506	-9.442\pm7.409 (99%), lag=0, P=0.001	1.070\pm1.071 (99%), lag=7, P=0.010

18